

# DEVELOPMENT OF IH ACCELERATING STRUCTURES WITH PMQ FOCUSING FOR LOW-BETA ION BEAMS

S.S. Kurennoy, J.F. O'Hara, E.R. Olivas, L.J. Rybarczyk, LANL, Los Alamos, NM 87545, U.S.A.

## Abstract

We are developing high-efficiency room-temperature RF accelerating structures based on inter-digital H-mode (IH) cavities and the transverse beam focusing with permanent-magnet quadrupoles (PMQ), for beam velocities in the range of a few percent of the speed of light. Such IH-PMQ accelerating structures following a short RFQ can be used in the front end of ion linacs or in stand-alone applications such as a compact deuteron-beam accelerator up to the energy of several MeV. New results from our detailed electromagnetic 3-D modeling combined with beam dynamics simulations and thermal-stress analysis for a complete IH-PMQ accelerator tank, including the end-cell design, are presented.

## INTRODUCTION

Room-temperature accelerating structures based on inter-digital H-mode (IH) resonators are especially efficient at very low beam velocities,  $\beta = v/c < 0.1$ . Small sizes of the drift tubes (DTs), which are required for achieving high shunt impedances in the H-resonators, usually prevent placing conventional electromagnetic quadrupoles inside DTs. Inserting permanent-magnet quadrupoles (PMQs) inside small DTs of the H-structure, as was suggested in [1], promises both efficient beam acceleration and good transverse focusing. Further studies of this approach in [2, 3], based on electromagnetic 3-D modeling, beam-dynamics simulations, and engineering analysis, confirmed that IH-PMQ accelerating structures are feasible. Papers [2, 3] studied only one or a few periods of the IH structures in the beam velocity range  $\beta = 0.0325-0.065$ , corresponding to the deuteron beam energies from 1 to 4 MeV.

In this paper we consider a short tank containing the IH-PMQ accelerating structures with vanes. The range of the design beam velocities is  $\beta = 0.0325-0.05$ , so that the tank can serve as the first of two tanks in a 1-4 MeV compact deuteron accelerator. We concentrate mostly on the end-cell design and the means to tune the electric field profile along the beam axis, as well as the frequency of the working mode to 201.25 MHz.

## IH-TANK DESIGN

The magnetic field of the  $TE_{11(0)}$  mode, the working mode of IH resonators, is directed along the beam axis on one side of the DTs, their supporting stems, and vanes (if any), and in the opposite direction on the other side of the DTs-stems. In other words, the magnetic field lines form a loop around the DTs and stems in the plane containing the beam axis and transverse to the stems. The field magnitude is almost constant in the resonator transverse cross section [4]. There should be some space between the

DTs/vanes and the end walls for the magnetic flux to turn around; this defines the design requirement for the tank end cells.

## Tank Layout

The layout of a short tank containing IH structures with vanes is presented in Figs. 1-2. Figure 1 shows only the IH DTs, supporting stems, and vanes. In Fig. 2 the longitudinal cross section of the tank is shown; the blue line indicates the beam axis. The cell length  $L_c$  increases along the structure as  $L_c = \beta_g \lambda / 2$ , where  $\beta_g$  is the design beam velocity and  $\lambda$  is the RF wavelength; see in Fig. 2.

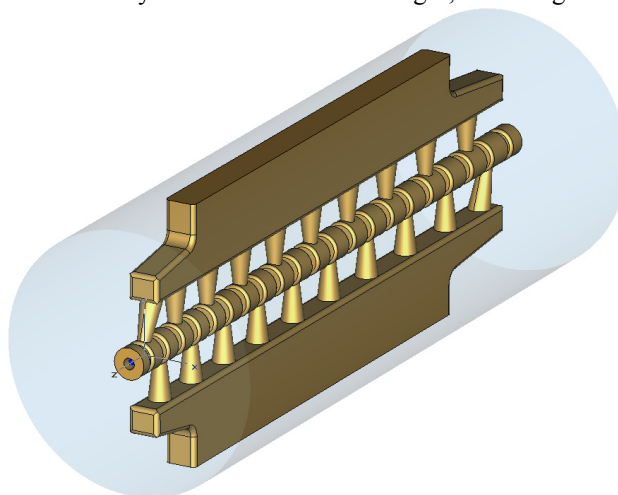


Figure 1: MWS model of a short IH tank. The outer wall is removed; the cavity inner volume is in light-blue.

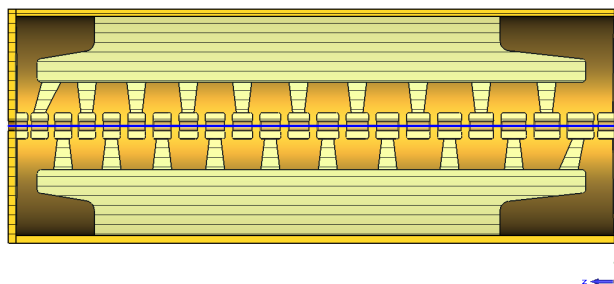


Figure 2: Cross section of the IH tank with the outer wall.

This tank contains 10 IH “periods”; an IH period consists of two cells. Each cell includes one DT that can house a PMQ, and two half-DTs are located on the end walls. Some tank dimensions are presented in Tab. 1.

Table 1: Dimensions of the IH Tank

Dimension	Value
Tank inner-cavity length $L$ , cm	62.97
Inner radius of the tank cavity $R$ , cm	11.52
DT length min / max, cm	1.81 / 2.84
DT aperture radius / outer radius, cm	0.5 / 1.4

### Results of Electromagnetic (EM) Modeling

EM modeling was performed with the CST MicroWave Studio (MWS) [5]. The magnitude of the on-axis electric field in the IH tank is shown in Fig. 3, for the accelerating gradient  $E_0 = 2.5$  MV/m. The next closest mode – TE<sub>11(1)</sub> longitudinal harmonic, with one node in the middle of the tank – is at  $\approx 224$  MHz, 23 MHz above the working mode.

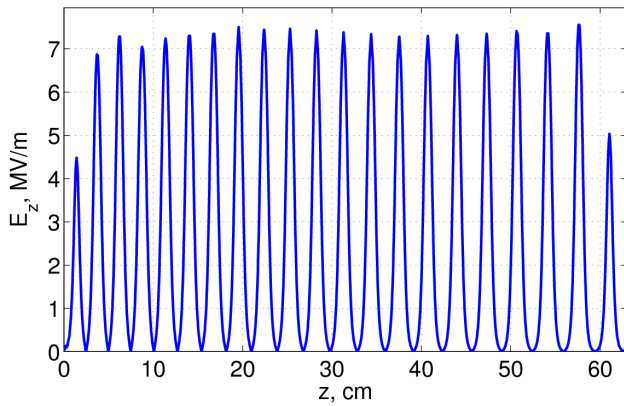


Figure 3: Electric field profile along the tank.

The field profile with the most of inner gaps having the same width,  $g = 8$  mm, and with the vane undercuts [4] is relatively flat. The widths of a few end gaps were reduced to 3.3, 6.8, and 6.8 mm in the upstream end (left in Fig. 2) and to 7.25 and 4.25 mm in the downstream end, to bring up the on-axis fields there; still the end-gap fields are lower than in the inner gaps. The magnitude of the electric field in a gap is rather sensitive to variations of the gap width: reducing  $g$  in the 11<sup>th</sup> gap (middle of the tank) by 1 mm increases the local on-axis field by almost 10%, without large changes elsewhere. The frequency sensitivity to this gap change is  $\Delta f/\Delta g \approx 0.4$  MHz/mm.

The calculated electromagnetic (EM) parameters of the tank are summarized in Tab. 2. A copper surface with the conductivity of  $5.8 \cdot 10^7$  1/Ω/m was assumed for RF loss calculations; the Kilpatrick field at 201.25 MHz is  $E_K = 14.8$  MV/m.

Table 2: EM parameters of the IH tank

Parameter	Value
Quality factor $Q$	9678
Transit-time factors $T$ (21 gaps)	0.88-0.94
Effective shunt impedance $ZT^2$ , MΩ/m	481
Surface RF power loss, kW *	13.4
Maximal electric field $E_{max}$ , MV/m	20.2 (1.37 $E_K$ )
Maximal surface loss density, W/cm <sup>2</sup> *	69.2

\* At 100% duty

The surface-current distribution on the inner tank surfaces is shown in Fig. 4, with the tank outer shell removed. The hottest spots are on the vane undercuts. The RF power loss is distributed over the tank elements as follows: 43.8% on the outer walls, 36.0% on the vanes, 13.8% on the stems, and only 6.3% on the DTs. This suggests that efficient water cooling of the tank can be achieved using cooling channels only inside the vanes and on the outer walls.

### Low and Medium Energy Accelerators and Rings

#### A08 - Linear Accelerators

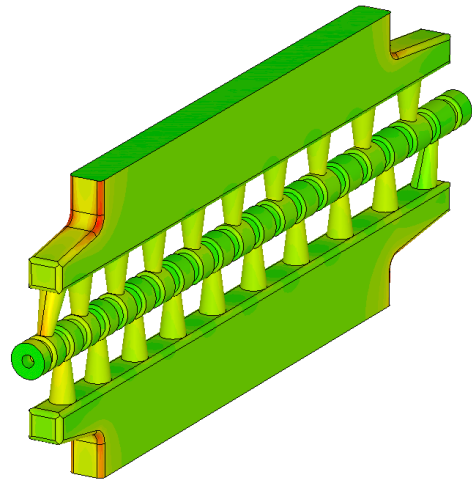


Figure 4: Distribution of surface-current magnitude: red color corresponds to the highest value, dark-green to zero.

We consider additional frequency and field-tilt slug tuners for the IH tank. A symmetrical pair of cylindrical slugs of 8-cm diameter in the middle of the tank shifts the cavity frequency by  $\Delta f/\Delta d \approx 0.77$  MHz/cm, where  $d$  is the tuner protrusion depth. The electric fields in the gaps near the tuners slightly decrease as the tuners move in. Two pairs of such slug tuners placed in the beginning and the end of the tank can provide a tilted field profile if needed. Moving the first pair of tuners in and the second one out by 1 cm creates a tilt of about 16%, with the lower fields in the beginning of the tank. The opposite tilt (high to low with the tuners out / in) is less pronounced, about 10%.

### Heating and Stress Analysis

The heat loads on the tank surfaces calculated by MWS were transferred into ANSYS [6] using a procedure that was developed earlier, see [2, 3], for a thermal-stress analysis. The tank is water-cooled using one channel in each vane and one U-shaped loop on each of the two end walls. The temperature distribution for the duty factor of 10% is shown in Fig. 5. One can see the PMQs (SmCo) in Fig. 5 as cylindrical insertions inside the DTs; they were taken into account in the thermal analysis. The inlet water is at 22°C, with the flow rate 2 gpm at velocity 4.5 m/s. For the 10% duty, the maximal temperature is 34.5°C on the first DT (red) while the minimal one is 23°C in the vanes (dark-blue).

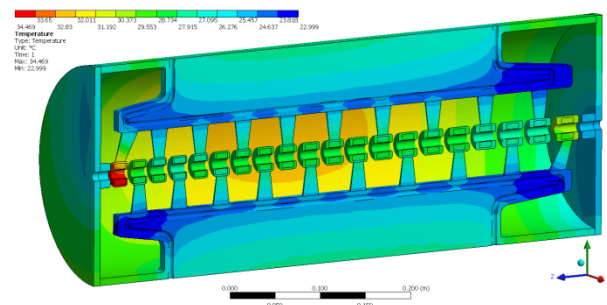


Figure 5: Temperature distribution at 10% duty. Cut-out view reveals the cooling channels inside the vanes.

The maximum reaches 41°C and 47°C at 15% and 20% duty, respectively, with the pattern similar to that in Fig. 5. It is important to emphasize that the proposed cooling in vanes is sufficient to keep the temperatures of the PMQs inside the DTs well below the maximal acceptable PMQ working temperature, 150-250°C, without need to cool the DTs and stems using dedicated channels.

The maximal structural stress at the duty factor of 10% is only 37 MPa near the vane-cover connection and can be further reduced by making a smooth blend there. The relative longitudinal DT displacements in the structure are small, below a few  $\mu\text{m}$ . There are some relative vertical displacements of the DTs supported by the opposite vanes, especially near the tank ends: about 48  $\mu\text{m}$  between the two first DTs (on the upstream end), and near 60  $\mu\text{m}$  for the last two DTs. These misalignments can be prevented by choosing the initial positions of these DTs with the correct vertical offsets, if beam dynamics simulations indicate that it is needed.

### Beam Dynamics Simulations

For the beam dynamics simulations, we assumed that each DT contains a PMQ. All PMQs are identical, with the inner radius 6 mm, outer radius 12 mm, and length 16 mm. The quadrupole gradient with SmCo was estimated to be 165 T/m. The field-overlap effect for the two close PMQs in the F-D configuration was calculated; it reduces the fields by less than 3% in the worst case. TRACE-3D [7] simulations indicated that the best transverse focusing is achieved when the PMQs are arranged to form an FFDD lattice, see in Fig. 6.

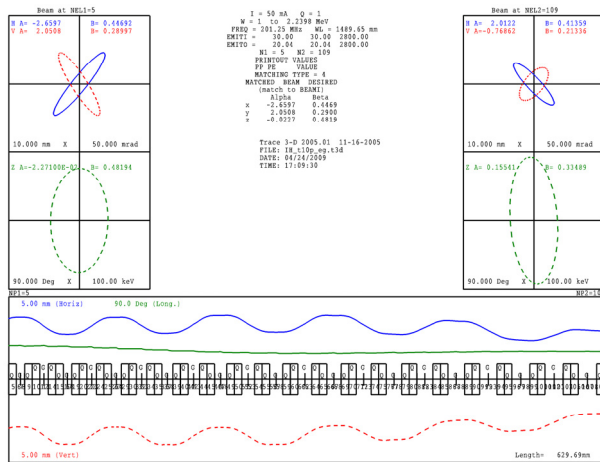


Figure 6: Output of TRACE-3D envelope calculations.

The distribution of the average accelerating gradient per gap corresponding to the electric field in Fig. 3 goes from high to low along the tank, due to the shorter periods in its upstream part. Multi-particle beam dynamics simulations were performed for a 50-mA deuteron beam with the initial normalized transverse emittance of  $0.2 \pi \text{ mm-mrad}$  at the source. First the beam propagation through a generic RFQ from 50 keV to 1 MeV was modeled with PARMTEQM [7]. The results were used to establish the

parameters for the input beam emittance in a beam-envelope simulation of the IH tank using TRACE-3D. Matching the input beam in the first full IH period produced the beam envelopes shown in Fig. 6. The synchronous RF phase for each gap was  $-30^\circ$ . We expect that a phase ramp in the upstream part of the tank will improve the beam dynamics. The phase ramp can be achieved by moving the DTs, while keeping the gap lengths fixed, in the longitudinal direction: to reduce the gap phase by  $15^\circ$ , the DT in the beginning of the tank should be moved upstream by less than 2.1 mm. Our future plans for beam dynamics studies include multi-particle simulations using 3-D RF and PMQ fields computed by the CST MW and EM Studio [5].

### SUMMARY

We presented the results of detailed electromagnetic 3-D modeling for the accelerator tank containing the IH-PMQ structure designed for the beam velocity range  $\beta = 0.0325\text{-}0.05$  at the frequency 201.25 MHz. The main focus was on the end-cell design and the means to tune the field profile along the tank, as well as the frequency and field-tilt sensitivity.

The thermal-stress analysis was performed with ANSYS. It demonstrated the feasibility of water-cooling the IH-PMQ tank employing the cooling channels in the vanes and on the tank end walls only, not in the stems or DTs. Beam dynamics simulations indicate the advantage of having a phase ramp along the tank. We plan to implement the phase ramp by moving the DTs, and then continue detailed multi-particle simulations using computed RF and PMQ 3-D fields.

This work is supported by the LANL Laboratory Directed R&D program (LDRD). The authors would like to thank D. Barlow and T. Wangler for help and useful discussions.

### REFERENCES

- [1] S. Kurennoy, L. Rybarcyk, and T. Wangler, "Efficient Accelerating Structures for Low-Energy Light Ions," PAC'07, Albuquerque, NM, p. 3824 (2007).
- [2] S. Kurennoy, S. Konecni, J. O'Hara, & L. Rybarcyk, "IH Accelerating Structures with PMQ Focusing for Low-Energy Light Ions," EPAC'08, Genoa, p. 3428 (2008).
- [3] S. Kurennoy, J. O'Hara, E. Olivas, and L. Rybarcyk, "Efficient Low-Beta H-mode Accelerating Structures with PMQ Focusing," Linac08, Victoria, BC, THP071 (2008).
- [4] U. Ratzinger, NIM A464 (2001) 636; Proceed. CAS 2000, CERN 2005-003, p. 351 (2005).
- [5] MicroWave Studio, CST, 2009, www.cst.com.
- [6] ANSYS, ANSYS Inc., www.ansys.com.
- [7] Los Alamos Accelerator Code Group (LAACG), LANL, laacg.lanl.gov.